LETTER

doi:10.1038/nature12193

Small effect of water on upper-mantle rheology based on silicon self-diffusion coefficients

Hongzhan Fei[1], Michael Wiedenbeck[2], Daisuke Yamazaki[3] & Tomoo Katsura[1]

Water has been thought to affect the dynamical processes in the Earth's interior to a great extent. In particular, experimental deformation results[1–4] suggest that even only a few tens of parts per million of water by weight enhances the creep rates in olivine by orders of magnitude. However, those deformation studies have limitations, such as considering only a limited range of water concentrations and very high stresses, which might affect the results. Rock deformation can also be understood as an effect of silicon self-diffusion, because the creep rates of minerals at temperatures as high as those in the Earth's interior are limited by self-diffusion of the slowest species[5,6]. Here we experimentally determine the silicon self-diffusion coefficient D_{Si} in forsterite at 8 GPa and 1,600 K to 1,800 K as a function of water content C_{H2O} from less than 1 to about 800 parts per million of water by weight, yielding the relationship, $D_{Si} \approx (C_{H2O})^{1/3}$. This exponent is strikingly lower than that obtained by deformation experiments (1.2; ref. 7). The high nominal creep rates in the deformation studies under wet conditions may be caused by excess grain boundary water. We conclude that the effect of water on upper-mantle rheology is very small. Hence, the smooth motion of the Earth's tectonic plates cannot be caused by mineral hydration in the asthenosphere. Also, water cannot cause the viscosity minimum zone in the upper mantle. And finally, the dominant mechanism responsible for hotspot immobility cannot be water content differences between their source and surrounding regions.

Diffusion creep and dislocation creep are two important mechanisms that dominate the plastic deformation of rocks and minerals in Earth's interior. Experimental deformation studies have suggested that incorporation of water in olivine significantly enhances both dislocation and diffusion creep rates[1–4,7]. However, we note that those studies used polycrystalline olivine samples with over-saturated water. In such samples, large amounts of free water may have existed on grain boundaries, leading to a large enhancement of grain boundary sliding (or pressure-solution-accommodated creep), rather than dislocation creep or diffusion creep in the grain interior. On the other hand, the upper mantle is water unsaturated and free water is unlikely to exist. Therefore, the enhancement of creep rates by free water cannot occur in the real upper mantle. We also note that the ranges of water contents ($C_{H2O} < 80$ wt p.p.m.) in these deformation studies[1–4,7] are too narrow to determine accurately the effect of water on stress–strain rate measurements. This can lead to large errors in estimating the effect of water on mantle rheology.

Another problem with such rock deformation experiments is the very high stress (typically a hundred times higher than that in Earth's interior) needed to obtain experimentally determinable strain rates. High stress causes anomalously high-density dislocations, stacking faults and sub-grain boundaries, which may lead to artificial results for the Earth's interior. Instead, the measurement of self-diffusion coefficients in minerals is an independent way to study mantle rheology because high-temperature mineral creep is believed to be controlled by self-diffusion of the slowest species[5,6] (which is silicon in the case of olivine[8,9]). It allows a much wider range of experimental conditions (such as pressure and C_{H2O}) and also does not induce unrealistically high defect densities.

Costa and Chakraborty[8] measured silicon self-diffusion coefficients (D_{Si}) in olivine single crystals with C_{H2O} values of ~40 and 370 parts per million by weight (wt p.p.m.) and concluded that even 45 wt p.p.m. of water enhances D_{Si} by two to three orders of magnitude by comparison with the results obtained under dry conditions by ref. 10. However, the data of ref. 8 did not show a systematic change in D_{Si} with C_{H2O} at ~40 and at ~370 wt p.p.m. In addition, our previous study[11] showed that ref. 10 may have underestimated D_{Si} under dry conditions. We therefore propose that the water effect was overestimated in ref. 8.

Here we systematically measured D_{Si} in olivine as a function of C_{H2O}. Because the effects of iron on D_{Si} and on creep rates are very small under upper-mantle conditions[11,12], a single-crystal forsterite sample was used. We measured its D_{Si} at 8 GPa, 1,600 K and 1,800 K, and with well controlled C_{H2O} from <1 up to about 800 wt p.p.m., which is realistic for the oceanic mantle. The experimental details are given in the Methods section.

Experimental results are shown in Fig. 1. D_{Si} systematically increases with increasing C_{H2O}. D_{Si} values under wet conditions ($C_{H2O} > 1$ wt p.p.m.) were fitted to the Arrhenius equation:

$$D_{Si} = A_0 C_{H2O}^{r} \exp\left(-\frac{\Delta H}{RT}\right) \quad (1)$$

where A_0 is the pre-exponential factor, r is the C_{H2O} exponent, R is the gas constant, T is the absolute temperature, and ΔH is the activation

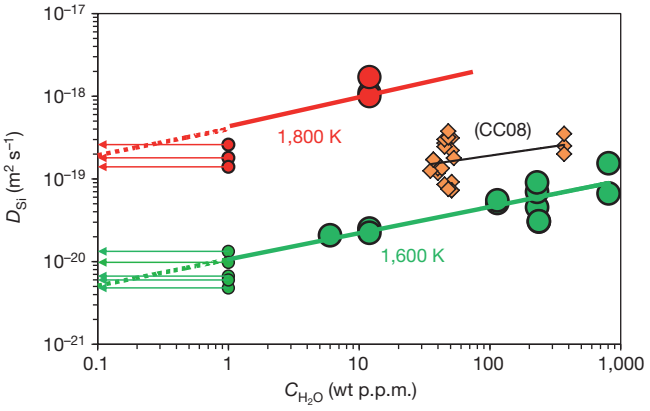

Figure 1 | D_{Si} versus C_{H2O} at 1,600 K and 1,800 K. The data points shown by small circles with an arrow are taken from ref. 11 on D_{Si} in dry forsterite at 8 GPa, with $C_{H2O} < 1$ wt p.p.m.; these are below the detection resolution of FT-IR and SIMS. It was impossible to obtain data points at 1,800 K with high C_{H2O} because of the low melting temperature of hydrous forsterite[31]. Even when C_{H2O} was low, the isotopically enriched thin-film coating of the diffusion couple was often damaged during annealing at this temperature. CC08 indicates data points (orange diamonds) taken from Costa and Chakraborty[8], normalized to 1,600 K and 8 GPa, using an activation energy of 358 kJ mol^{-1} from ref. 8 and an activation volume of 1.7 cm^3 mol^{-1} from ref. 11.

[1]Bayerisches Geoinstitut, Universität Bayreuth, Bayreuth D95440, Germany. [2]Helmholtz Centre Potsdam, Potsdam D14473, Germany. [3]Institute for Study of the Earth's Interior, Okayama University, Misasa, Tottori 682-0193, Japan.

enthalpy. By fitting the experimental results to equation (1), we determined A_0, r and ΔH to be $10^{-5.8\pm0.7}\,m^2\,s^{-1}$, 0.32 ± 0.07 and $434\pm20\,kJ\,mol^{-1}$, respectively. The activation energy ΔE is $420\pm23\,kJ\,mol^{-1}$ (after a pressure correction using an activation volume of $1.7\pm0.4\,cm^3\,mol^{-1}$; ref. 11), which is essentially the same as that for dry conditions ($410\pm30\,kJ\,mol^{-1}$; see Supplementary Information)[11].

The present results thus demonstrate $D_{Si}\propto(C_{H2O})^{0.32\pm0.07}\approx(C_{H2O})^{1/3}$. Given that $[V_{Si}'''']$ (where four primes indicates a charge of minus four on the Si vacancies) is proportional to $(C_{H2O})^{2/3}$ (ref. 13) under the charge-neutral conditions (where the dot indicates one positive charge on the hydroxide ion on the oxygen site), $[(OH)_O^{\bullet}]=2[V_{Mg}'']$ (ref. 14), a special explanation is necessary for the C_{H2O} exponent of D_{Si}. One hypothesis accounting for the C_{H2O} exponent is that Si diffusion is controlled by $V_O^{\bullet\bullet}$ as well as V_{Si}''''. The Si^{4+} in forsterite is tightly surrounded by O^{2-} in a tetrahedron. If an oxygen ion is missing, the hopping probability of V_{Si}'''' should greatly increase. Hence, Si diffusion may be dominated by $V_O^{\bullet\bullet}$-associated V_{Si}''''. Although the $[V_O^{\bullet\bullet}]$ is low, a certain proportion of V_{Si}'''' should be associated with $V_O^{\bullet\bullet}$ owing to the Coulomb potential. As a result, D_{Si} should be proportional to both $[V_{Si}'''']$ and $[V_O^{\bullet\bullet}]$. Given that $[V_O^{\bullet\bullet}]\propto(C_{H2O})^{-1/3}$ (ref. 13), we have $D_{Si}\propto[V_{Si}'''']\times[V_O^{\bullet\bullet}]\propto(C_{H2O})^{2/3}\times(C_{H2O})^{-1/3}=(C_{H2O})^{1/3}$. However, we do not know what proportion of V_{Si}'''' is associated with $V_O^{\bullet\bullet}$. It is possible that all the V_{Si}'''' are associated with $V_O^{\bullet\bullet}$ because of the high Coulomb potential. In this case, D_{Si} would not be proportional to $[V_O^{\bullet\bullet}]$. Further investigation is required to explain the observed small C_{H2O} exponent of D_{Si} in view of defect chemistry.

Natural iron-bearing olivine in the real mantle can contain small amounts of $Fe_{Me}^{\bullet}$, (where Fe^{3+} on a Fe or Mg metal site has an excess charge of +1) which may change the charge neutrality conditions and the C_{H2O} exponents for D_{Si}. However, the D_{Si} obtained in natural olivine by ref. 8 under wet conditions at high pressure showed essentially the same increase with increasing C_{H2O} from 30–50 wt p.p.m. to 370 wt p.p.m., as shown in Fig. 1. It suggests that $Fe_{Me}^{\bullet}$ in natural olivine is not essential for Si diffusion in the investigated C_{H2O} range.

In the case that C_{H2O} is extremely high, the defect chemistry could be changed by incorporation of protons in Si vacancies and the hydrated Si vacancies—H_{Si}''', $(2H)_{Si}''$, $(3H)_{Si}'$ and $(4H)_{Si}^{\times}$) (where the superscript cross indicates no excess charge on the Si vacancy)—whose concentrations have a larger C_{H2O} exponent (that is, 0.5–2) than V_{Si}'''' (ref. 13), could dominate Si diffusion, possibly leading to a hydrolytic weakening of olivine[15]. For this reason, we expect D_{Si} to have a larger C_{H2O} exponent under high C_{H2O} conditions. However, our experimental results do not show an increase in the C_{H2O} exponent up to 800 wt p.p.m. Higher C_{H2O} conditions are unlikely in the upper mantle except for in the mantle wedge, judging from petrological studies (~70–160 wt p.p.m. of water in depleted mantle[16], and a value four to five times higher in enriched mantle[17,18]). Therefore, the C_{H2O} exponent of 1/3 is the maximum for the majority of the upper mantle.

Diffusion creep and dislocation creep in olivine under high temperatures are thought to be controlled by Si self-diffusion[5,6]. Therefore, the C_{H2O} exponent for D_{Si} should be identical to that for creep rates. However, deformation studies[1–4,7] on olivine aggregates claimed a much larger C_{H2O} exponent, 1.2 ± 0.4 (Fig. 2). We found that the infrared spectra in these studies[1–3] showed tiny sharp peaks with a broad band. This suggests that most of the water existed on grain boundaries. Accordingly, the high strain rates in their wet samples might have been caused by grain boundary sliding enhanced by free water on grain boundaries (see further discussion in the Supplementary Information). This idea is also supported by the much lower creep rates obtained in single crystals of hydrous olivine[19] than those in polycrystalline (Fig. 2). Free water is unlikely to be present in the upper mantle (except for the mantle wedge), owing to the water-unsaturated conditions. In addition, the grain size is on the order of millimetres to centimetres in the upper mantle[20], meaning grain boundary sliding would be negligible[7]. Therefore, the creep rates of minerals in the real mantle cannot be enhanced by free water on grain boundaries.

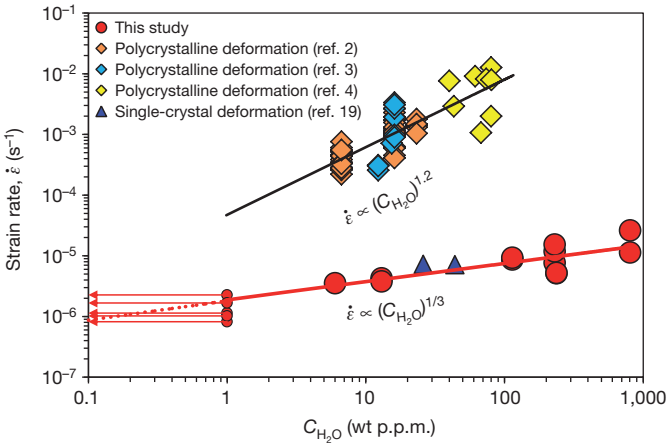

Figure 2 | Strain rate versus C_{H2O}. D_{Si} values from this study are converted to strain rate using the proportional relationship of D_{Si} and strain rate[6] with parameters from ref. 13. All data are normalized to a pressure of 8 GPa, a temperature of 1,600 K, and a stress of 300 MPa using an activation volume of $1.7\,cm^3\,mol^{-1}$ (ref. 11), activation energy of $420\,kJ\,mol^{-1}$, and a stress exponent of 3.5. The data points for $C_{H2O}<1$ wt p.p.m. are treated in the same way as in Fig. 1.

Based on the small C_{H2O} exponent ($r=1/3$) determined in this study, the difference in D_{Si}, as well as creep rates, between rheologically dry (<1 wt p.p.m.) and maximum C_{H2O} of olivine in upper mantle (<1,000 wt p.p.m.; refs 16–18) is within one order of magnitude. Because the variance of C_{H2O} in the upper mantle is very small, that is, ~100–1,000 wt p.p.m. (refs 16–18), such a small range only causes ~0.3 orders of magnitude difference in creep rates. This is much smaller than other factors that affect rheological properties like temperature or shear stress. Hence, we conclude that the effect of water on upper mantle rheology is not significant, which is in complete contrast to what has been commonly accepted to be the case[7,8,21,22].

This small effect of water on upper-mantle rheology means that many geodynamical problems must be reconsidered. Two ideas, partial melting and hydration[7,21–23], have been commonly considered to explain plate motion because both could soften the oceanic asthenosphere. Previous overestimates of water effects on creep rates have erroneously supported the idea that hydration is the main reason for plate motion[7,21,22]. Using the C_{H2O} exponent of 1/3, if 75% of the original water is extracted during mantle dehydration (~110 wt p.p.m. of water before dehydration[16], and ~28 wt p.p.m. after dehydration[24]), the creep rates change only by a factor of 1.6. On the other hand, the melt fraction in the asthenosphere is estimated to be 1.25–0.25% (ref. 25) or less[26]. Such a small melt fraction enhances the creep rates by at most a factor of three[23]. However, the high geothermal gradient in the oceanic mantle at <200 km, and especially at <100 km (about $12\,K\,km^{-1}$)[27], causes the creep rates to increase by at least six orders of magnitude from a depth of 60 km to a depth of 200 km. Thus, the effect of temperature gradient on creep rates appears to be much larger than that of C_{H2O} or melt fraction. The softening of the oceanic asthenosphere that allows plate motion cannot occur by hydration or by partial melting.

In addition, the presence of a minimum-viscosity zone has been expected in the asthenosphere based on the seismically observed low-velocity and high-attenuation zone[28]. However, because the effect of pressure on D_{Si} is also small[11], the viscosity in the upper mantle (which is calculated using the inverse relationship between D_{Si} and viscosity[29] based on oceanic geotherm[27]) decreases monotonically with increasing depth (Fig. 3) even if the geothermal gradient is very small (that is, $<1\,K\,km^{-1}$) at a depth exceeding 200 km. Thus, on the basis of the values of D_{Si} and taking the effects of pressure, temperature, and

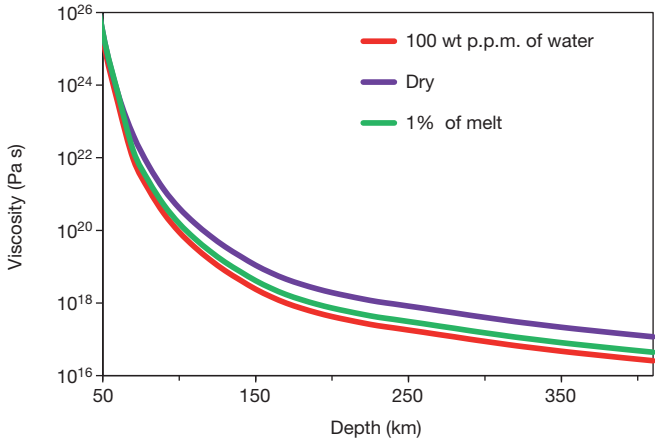

Figure 3 | Viscosity in the upper mantle. Viscosity η is calculated from D_{Si} using the inverse relationship of η and D_{Si} (ref. 29), that is, $\eta = 10kTr_c^2/(D_{Si}m_a)$, where k is the Boltzmann constant, T is the absolute temperature based on the oceanic geotherm[27], r_c is the crystal radius, and m_a is the mass of a Si ion. The grain size in the mantle is assumed to be ~1 mm. D_{Si} is a function of temperature, C_{H2O} and pressure, as given by equation (1) with $\Delta H = \Delta E + P\Delta V$, for which activation energy ΔE and activation volume ΔV values of 420 kJ mol^{-1} and 1.7 cm^3 mol^{-1} were used[11], respectively. The influence of partial melting on viscosity is calculated from the melt fraction dependence of creep rates[23].

water content into account, the minimum-viscosity zone does not appear in the asthenosphere.

Finally, an open question in mantle dynamics is why hotspots are so immobile in the face of plate motion. If it were true that water has a large effect on mantle rheology, high values of C_{H2O} in the source regions of hotspots in comparison to that in surrounding regions would be a possible explanation. However, our results demonstrate that this idea is not valid. Taking the Hawaii hotspot as an example, the C_{H2O} in its source is ~750 wt p.p.m., and ~110 wt p.p.m. in the surrounding regions[17]. Our results indicate that this difference would cause a viscosity contrast of a factor of two, which is rather small in comparison with that caused by temperature difference (~200 K hotter than surrounding mantle[30], resulting in a viscosity decrease by more than one order of magnitude). Hence, the C_{H2O} contrast cannot be the major reason for the immobility of hotspots.

METHODS SUMMARY

A synthetically produced forsterite single crystal was cored into disks with diameter 1 mm and thickness 1 mm, which were used as the starting materials. The chemical composition of the crystal was Mg_2SiO_4 with Ir the major impurity (~80 wt p.p.m.). The cored disks were doped with water at 8 GPa and 1,600 K using talc + brucite as a water source with enstatite + graphite/gold powder, using a multi-anvil apparatus. The variation of water contents in the samples were made by varying the ratio of the water source to the enstatite + graphite/gold powder. After being carefully polished in an alkaline colloidal silica solution, each water-doped disk was coated with a ~500 nm ^{29}Si-enriched Mg_2SiO_4 thin film by a pulsed laser deposition system, and then annealed at 8 GPa and 1,600 K or 1,800 K for diffusion. The water contents in the samples were determined using Fourier transform infrared (FT-IR) spectroscopy both before and after diffusion annealing. The sample surfaces with the thin film were polished again in the alkaline solution after diffusion annealing to reduce their surface roughness, which could lead to large analytical uncertainties in diffusion profile analyses. The diffusion profiles were obtained using a Cameca 6f secondary ion mass spectrometer (SIMS). The diffusion coefficients were calculated by fitting the profiles to the solution of Fick's second law.

Full Methods and any associated references are available in the online version of the paper.

Received 31 August 2012; accepted 12 April 2013.

1. Mei, S. & Kohlstedt, D. L. Influence of water on plastic deformation of olivine aggregates. 1. Diffusion creep regime. *J. Geophys. Res.* **105,** 21457–21469 (2000).
2. Mei, S. & Kohlstedt, D. L. Influence of water on plastic deformation of olivine aggregates. 2. Dislocation creep regime. *J. Geophys. Res.* **105,** 21471–21481 (2000).
3. Karato, S. I., Paterson, M. S. & Fitzgerald, J. D. Rheology of synthetic olivine aggregates: influence of grain size and water. *J. Geophys. Res.* **91,** 8151–8176 (1986).
4. Jung, H. & Karato, S. Water-induced fabric transitions in olivine. *Science* **293,** 1460–1463 (2001).
5. Frost, H. J. & Ashby, M. F. *Deformation Mechanism Maps* Ch. 2 6–16 (Pergamon Press, 1982).
6. Weertman, J. in *Mechanics and Materials: Fundamentals and Linkages* (eds Meyers, M. A., Armstrong, R. W. & Kirschner, H.) 451–488 (Wiley, 1999).
7. Hirth, G. & Kohlstedt, D. L. Rheology of the upper mantle and the mantle wedge: a view from the experimentalists. *Geophys. Monogr. Ser.* **138,** 83–105 (2003).
8. Costa, F. & Chakraborty, S. The effect of water on Si and O diffusion rates in olivine and implications for transport properties and processes in the upper mantle. *Phys. Earth Planet. Inter.* **166,** 11–29 (2008).
9. Houlier, B., Cheraghmakani, M. & Jaoul, O. Silicon diffusion in San Carlos olivine. *Phys. Earth Planet. Inter.* **62,** 329–340 (1990).
10. Dohmen, R., Chakraborty, S. & Becker, H. W. Si and O diffusion in olivine and implications for characterizing plastic flow in the mantle. *Geophys. Res. Lett.* **29,** 2030, http://dx.doi.org/10.1029/2002GL015480 (2002).
11. Fei, H. *et al.* High silicon self-diffusion coefficient in dry forsterite. *Earth Planet. Sci. Lett.* **345–348,** 95–103 (2012).
12. Durham, W. B. & Goetze, C. A comparison of the creep properties of pure forsterite and iron-bearing olivine. *Tectonophysics* **40,** T15–T18 (1977).
13. Kohlstedt, D. L. The role of water in high-temperature rock deformation. *Rev. Mineral. Geochem.* **62,** 377–396 (2006).
14. Kohlstedt, D. L., Keppler, H. & Rubie, D. C. Solubility of water in the α, β and γ phases of $(Mg,Fe)_2SiO_4$. *Contrib. Mineral. Petrol.* **123,** 345–357 (1996).
15. Brodholt, J. P. & Refson, K. An ab initio study of hydrogen in forsterite and a possible mechanism for hydrolytic weakening. *J. Geophys. Res.* **105,** 18977–18982 (2000).
16. Workman, R. K. & Hart, S. R. Major and trace element composition of the depleted MORB mantle (DMM). *Earth Planet. Sci. Lett.* **231,** 53–72 (2005).
17. Dixon, J. E., Leist, L., Langmuir, C. & Schilling, J. G. Recycled dehydrated lithosphere observed in plume-influenced mid-ocean-ridge basalt. *Nature* **420,** 385–389 (2002).
18. Hirschmann, M. M. Water, melting, and the deep Earth H_2O cycle. *Annu. Rev. Earth Planet. Sci.* **34,** 629–653 (2006).
19. Raterron, P. *et al.* Experimental deformation of olivine single crystals at mantle pressures and temperatures. *Phys. Earth Planet. Inter.* **172,** 74–83 (2009).
20. Karato, S. I. Grain-size distribution and rheology of the upper mantle. *Tectonophysics* **104,** 155–176 (1984).
21. Hirth, G. & Kohlstedt, D. L. Water in the oceanic upper mantle: implications for rheology, melt extraction and the evolution of the lithosphere. *Earth Planet. Sci. Lett.* **144,** 93–108 (1996).
22. Karato, S. I. & Jung, H. Water, partial melting and the origin of the seismic low velocity and high attenuation zone in the upper mantle. *Earth Planet. Sci. Lett.* **157,** 193–207 (1998).
23. Mei, S., Bai, W., Hiraga, T. & Kohlstedt, D. L. Influence of melt on the creep behavior of olivine–basalt aggregates under hydrous conditions. *Earth Planet. Sci. Lett.* **201,** 491–507 (2002).
24. Bell, D. R. & Rossman, G. R. Water in Earth's mantle: the role of nominally anhydrous minerals. *Science* **255,** 1391–1397 (1992).
25. Kawakatsu, H. *et al.* Seismic evidence for sharp lithosphere-asthenosphere boundaries of oceanic plates. *Science* **324,** 499–502 (2009).
26. Hirschmann, M. M. Partial melt in the oceanic low velocity zone. *Phys. Earth Planet. Inter.* **179,** 60–71 (2010).
27. Green, D. H. & Ringwood, A. E. The genesis of basaltic magmas. *Contrib. Mineral. Petrol.* **15,** 103–190 (1967).
28. Anderson, D. L. Earth's viscosity. *Science* **151,** 321–322 (1966).
29. McKenzie, D. P. The viscosity of the mantle. *Geophys. J. R. Astron. Soc.* **14,** 297–305 (1967).
30. Putirka, K. D. Mantle potential temperatures at Hawaii, Iceland, and the mid-ocean ridge system, as inferred from olivine phenocrysts: evidence for thermally driven mantle plumes. *Geochem. Geophys. Geosyst.* **6,** Q05L08 (2005).
31. Inoue, T. Effect of water on melting phase relations and melt composition in the system Mg_2SiO_4-$MgSiO_3$-H_2O up to 15 GPa. *Phys. Earth Planet. Inter.* **85,** 237–263 (1994).

Supplementary Information is available in the online version of the paper.

Acknowledgements We thank S. Chakraborty and R. Dohmen at Ruhr-University of Bochum for thin-film deposition and discussions about experimental methods. We also thank A. Yoneda at Okayama University for providing the single crystal, H. Keppler for FT-IR measurement, A. Audétat for ICP-MS analysis, and T. Boffa-Ballaran for X-ray diffraction analysis. We acknowledge support from the ENB (Elite Network Bavaria) programmes.

Author Contributions T.K. organized the project. The samples were prepared by H.F. and D.Y. All high pressure experiments and FT-IR measurements were performed by H.F. SIMS analyses were made by H.F. and M.W. The manuscript was completed by H.F. and T.K.; all authors read and commented on the manuscript.

Author Information Reprints and permissions information is available at www.nature.com/reprints. The authors declare no competing financial interests. Readers are welcome to comment on the online version of the paper. Correspondence and requests for materials should be addressed to H.F. (hongzhan.fei@uni-bayreuth.de).

METHODS

Starting material. A single-crystal forsterite sample was obtained from Oxide Company, Japan. The chemical composition of the crystal is Mg_2SiO_4. Its trace-element compositions were obtained from ref. 11. No O–H absorption bands were detected by Fourier transform infrared (FT-IR), indicating that the water content was less than 1 wt p.p.m. We used disks cored from the crystal, with diameter 1 mm and thickness 1 mm and the thickness oriented along the *b* axis.

Water-doping experiments. The cored forsterite disks were pre-annealed at 8 GPa and 1,600 K in the presence of a water source. This step is necessary to equilibrate the water in the crystal before diffusion annealing.

Each forsterite disk was loaded into a platinum capsule, with an outer diameter of 2.0 mm and an inner diameter of 1.6 mm, with one end sealed. A mixture of talc and brucite powders (weight ratio 4:1) was used as the water source and also to control the silica activity in the capsule. The space between the forsterite disk and capsule wall was filled with graphite or gold + enstatite (weight ratio 35:1) powder for low- and high-water-content experiments, respectively, to protect the single crystal from mechanical damage at high pressure (Supplementary Fig. 1). The capsule was closed and sealed by arc welding in liquid nitrogen to minimize water escape from the capsule. The water content in the capsule was controlled by the ratio of water source to graphite or gold + enstatite. In dry experiments, graphite powder was loaded around the samples; the capsules were then dried in a vacuum oven at 470 K for at least 24 h and sealed on a hot plate to minimize the amount of moisture absorbed from the atmosphere. The final length of capsules was 4–4.5 mm.

High-pressure experiments were performed using a Kawai-type multi-anvil apparatus at the University of Bayreuth. All experiments were performed at 8 GPa and 1,600 K. In each run, the sealed platinum capsule was located in an MgO cylinder in a $LaCrO_3$ stepped heater with a ZrO_2 thermal insulator. A MgO octahedron (with 5 wt% Cr_2O_3) with edge length 14 mm was used as the pressure medium (Supplementary Fig. 1). Eight tungsten carbide cubes with 32-mm edge length and 8-mm truncation edge length were used to generate high pressures. The temperatures were measured using a W97%Re3%-W75%Re25% thermocouple, 0.25 mm in diameter, whose junction was placed at the bottom of the capsule. The assembly was compressed to the target pressure over 2–4 h, heated to 1,273 K at a rate of 50 K min^{-1}, kept at 1,273 K for 1 h to decompose talc and brucite and to make the water distribution homogenous in the capsule, the assembly was then heated to 1,600 K in 5 min and kept for a long duration for water equilibration (50–70 h), as calculated from the hydrogen diffusion coefficients in forsterite[32]. The temperature was under automatic control, thus limiting variation to less than 2 K during annealing. After annealing, the sample was quenched by switching off the heating power and gradually decompressed to ambient pressure over a long period (15–20 h) to prevent crystal breakage.

The forsterite disks were recovered by cutting into the platinum capsule using a steel blade. No obvious cracks were found in the samples if small amounts of water source were used. With high amounts of water source, the crystal always contained some cracks and broke into pieces. However, in such cases we were still able to find usable pieces for diffusion experiments.

Deposition. The water-doped samples were polished using diamond powders with grain sizes of 0.25 μm, followed by an alkaline colloidal silica solution for >3 h until all small scratches were removed. The highly polished surface was then coated with ~500 nm of ^{29}Si enriched Mg_2SiO_4 and 100 nm of ZrO_2 using a pulsed laser deposition system at the Ruhr-University of Bochum[33]. We also conducted some diffusion experiments without the ZrO_2 film for comparison, and showed that the ZrO_2 does not affect D_{Si}, which was already confirmed in our previous study[11]. Prior to each deposition, the samples were heated up to 470 K for 10–15 min in the vacuum chamber of the pulsed laser deposition system so as to remove any free water from the sample surface. The structural water in the crystals did not escape during this step.

Diffusion annealing. Each thin-film-coated sample was placed in a platinum capsule with the same ratio of water source and graphite or gold + enstatite as used for the corresponding water-doping experiment and was then annealed at 8 GPa and 1,600 K or 1,800 K using the same high-pressure assembly (Supplementary Fig. 1). The annealing durations, ranging from 5–41 h as summarized in Supplementary Table 1, were estimated from silicon diffusion coefficient data for olivine[8] and forsterite[11].

FT-IR analysis. The water contents in the samples after water-doping experiments and also after diffusion annealing were measured using a high-resolution FT-IR spectrometer at the University of Bayreuth, described in ref. 11. Each forsterite sample for FT-IR analysis was polished on both faces normal to the *b* axis using 0.25-μm diamond powder. Two hundred scans were accumulated for each spectrum at a resolution of 1 cm^{-1}. Two or three spectra were obtained for each sample with at least one near the centre of the disk and one near the edge. One sample (V720) was also polished parallel to the *b* axis, and the water content was obtained as a function of distance from the coated thin film at 60-μm steps. After a background baseline correction and thickness normalization to 1 cm, the water contents were determined using the calibration given by[34]

$$C_{H2O} = 0.188 \times \int k(\nu)\mathrm{d}\nu \qquad (2)$$

where C_{H2O} was the water content in wt p.p.m. and $k(\nu)$ was the absorption coefficient at wavenumber ν. Integration was performed between 3,000 cm^{-1} and 4,000 cm^{-1} (ref. 11). The results of C_{H2O} in the samples are shown in the Supplementary Information.

SIMS analysis. The apparent diffusion profiles were measured by secondary ion mass spectrometry (SIMS) depth profiling using the Cameca IMS-6f installed at the Helmholtz Centre in Potsdam, Germany, with the same set-up for determining D_{Si} in dry forsterite as in our previous study[11]. The depth of each SIMS crater was determined using a 3D-Nanofocus vertical microscope at the University of Bayreuth. The D_{Si} was obtained by fitting the data to the solution of Fick's second law

$$c = \frac{c_0 - c_1}{2}\,\mathrm{erf}\left(\frac{x-h}{\sqrt{4Dt + L^2(\sigma)}}\right) + \frac{c_0 + c_1}{2} \qquad (3)$$

where c is the observed abundance of ^{29}Si, c_1 is the initial abundance of ^{29}Si in the isotopic film, c_0 is the initial abundance of ^{29}Si in the substrate, x is the distance from the surface, h is the position of the boundary between the thin film and substrate, t is the annealing time, $L(\sigma)$ is the nominal diffusion length in zero-time diffusion runs related to surface roughness (discussed below), and erf(z) is the error function[11]. An example of the diffusion profiles is shown in Supplementary Fig. 2.

Surface problem. Because of the crystallization of thin films, the surface roughness significantly increased during high-temperature annealing and became the major analytical uncertainty source[11]. Hence, the sample surfaces after diffusion annealing were chemically polished in an alkaline colloidal silica solution until the roughness was reduced to <50 nm, measured with a 3D-Nanofocus vertical microscope at University of Bayreuth. Only a thin layer (<200 nm), located well beyond the apparent diffusion profile, was removed during the final chemical polishing[11]. In addition, the apparent diffusion lengths obtained by SIMS were also corrected using a roughness calibration line obtained by a series of zero-time runs (equation (3)), in which the nominal diffusion lengths L are approximately a linear function of the standard deviation σ of the surface roughness at the bottoms of the craters (Supplementary Fig. 3). Detailed discussion about the surface problem is given in ref. 11.

32. Demouchy, S. & Mackwell, S. Water diffusion in synthetic iron-free forsterite. *Phys. Chem. Miner.* **30,** 486–494 (2003).
33. Dohmen, R. *et al.* Production of silicate thin films using pulsed laser deposition (PLD) and applications to studies in mineral kinetics. *Eur. J. Mineral.* **14,** 1155–1168 (2002).
34. Bell, D. R. *et al.* Hydroxide in olivine: a quantitative determination of the absolute amount and calibration of the IR spectrum. *J. Geophys. Res.* **108**(B2), 2105, http://dx.doi.org/10.1029/2001JB000679 (2003).